

RESEARCH ARTICLE

10.1002/2015JE004889

Key Points:

- Starkeyite $\text{MgSO}_4 \cdot 4\text{H}_2\text{O}$ is the best candidate for polyhydrated sulfate
- LH-1w formed by dehydration is the most likely form of the majority Martian $\text{MgSO}_4 \cdot \text{H}_2\text{O}$
- Key processes responsible for their coexistence are related to the metastability of starkeyite

Supporting Information:

- Supporting Information S1

Correspondence to:

A. Wang,
alianw@levee.wustl.edu

Citation:

Wang, A., B. L. Jolliff, Y. Liu, and K. Connor (2016), Setting constraints on the nature and origin of the two major hydrous sulfates on Mars: Monohydrated and polyhydrated sulfates, *J. Geophys. Res. Planets*, 121, 678–694, doi:10.1002/2015JE004889.

Received 6 JUL 2015

Accepted 28 JAN 2016

Accepted article online 2 FEB 2016

Published online 26 APR 2016

Setting constraints on the nature and origin of the two major hydrous sulfates on Mars: Monohydrated and polyhydrated sulfates

Alian Wang¹, Bradley L. Jolliff¹, Yang Liu², and Kathryn Connor¹

¹Department of Earth and Planetary Sciences and McDonnell Center for Space Sciences, Washington University, St. Louis, Missouri, USA, ²Southwest Research Institute, San Antonio, Texas, USA

Abstract Monohydrated Mg sulfate ($\text{MgSO}_4 \cdot \text{H}_2\text{O}$) and polyhydrated sulfate are the most common and abundant hydrous sulfates observed thus far on Mars. They are widely distributed and coexist in many locations. On the basis of results from two new sets of experiments, in combination with past experimental studies and the subsurface salt mineralogy observed at a saline playa (Dalangtan, DLT) in a terrestrial analogue hyperarid region on the Tibet Plateau, we can now set new constraints on the nature and origin of these two major Martian sulfates. Starkeyite ($\text{MgSO}_4 \cdot 4\text{H}_2\text{O}$) is the best candidate for polyhydrated sulfate. $\text{MgSO}_4 \cdot \text{H}_2\text{O}$ in the form of “LH-1w,” generated from dehydration of Mg sulfates with high degrees of hydration, is the most likely mineral form for the majority of Martian monohydrated Mg sulfate. Two critical properties of Mg sulfates are responsible for the coexistence of these two phases that have very different degrees of hydration: (1) the metastability of a substructural unit in starkeyite at relatively low temperatures, and (2) catalytic effects attributed to coprecipitated species (sulfates, chlorides, oxides, and hydroxides) from chemically complex brines that help overcome the metastability of starkeyite. The combination of these two properties controls the coexistence of the LH-1w layer and starkeyite layers at many locations on Mars, which sometimes occur in an interbedded stratigraphy. The structural H_2O held by these two broadly distributed sulfates represents a large H_2O reservoir at the surface and in the shallow subsurface on current Mars.

1. Introduction

Two important hydrous sulfates have been discovered on Mars by orbital remote sensing using the visible-near-infrared (Vis-NIR) reflectance spectrometers, the Observatoire pour la Minéralogie, l'Eau, les Glaces et l'Activité (OMEGA) onboard ESA's Mars Express [Bibring *et al.*, 2004] and the Compact Reconnaissance Imaging Spectrometer for Mars (CRISM) on board NASA's Mars Reconnaissance Orbiter [Murchie *et al.*, 2007]. The two hydrous sulfates are monohydrated Mg sulfate ($\text{MgSO}_4 \cdot \text{H}_2\text{O}$), which was identified on the basis of its distinct double band at 2.06 and 2.13 μm [Arvidson *et al.*, 2005; Gendrin *et al.*, 2005] and polyhydrated sulfate, whose nature remained largely undetermined hitherto because the observed spectral features match approximately with those of hydrous sulfates with a variety of cations and hydration degrees [Bibring *et al.*, 2005, 2006, 2007].

Two phenomena relevant to this finding of remote sensing are highly significant for Mars. First, monohydrated Mg sulfate $\text{MgSO}_4 \cdot \text{H}_2\text{O}$ (identified as kieserite in many remote sensing papers) and polyhydrated sulfates are the two most common hydrous sulfates, with the largest quantity and the widest distribution on the Martian surface (Figure 1). For instance, several kilometer thick layers of monohydrated and polyhydrated sulfates have been observed. Many of these layers are associated with the interior layered deposits (ILDs) in Valles Marineris near the equatorial region [Arvidson *et al.*, 2005; Bishop *et al.*, 2009; Catling *et al.*, 2006; Carter *et al.*, 2010; Dobrea *et al.*, 2008; Gendrin *et al.*, 2005; Flahaut *et al.*, 2010; Lichtenberg *et al.*, 2010; Massé *et al.*, 2008; Milliken *et al.*, 2008; Mangold *et al.*, 2008; Murchie *et al.*, 2009; Roach *et al.*, 2009, 2010; Weitz *et al.*, 2012; Wendt *et al.*, 2011], and additional occurrences have been found recently in other regions, including the Noachian southern highlands [Ackiss and Wray, 2014; Wray *et al.*, 2009, 2011; Wiseman *et al.*, 2010].

Other types of hydrated sulfates, especially Fe sulfates (e.g., jarosite, hydroxylated ferric sulfates, and szomolnokite) and Al sulfate (alunite), have been found by remote sensing either in low abundance (i.e., rarely identified) and/or occur only in localized spots [Bishop *et al.*, 2009; Farrand *et al.*, 2009; Lichtenberg *et al.*, 2010; Swayze *et al.*, 2008; Weitz *et al.*, 2012; Wray *et al.*, 2010, 2011]. Large quantity of gypsum have been

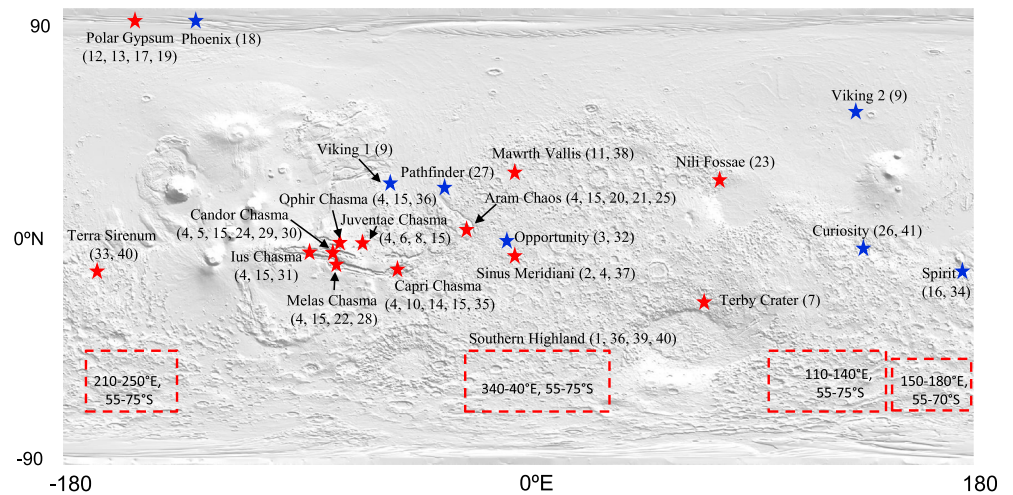


Figure 1. Locations on Mars where hydrous sulfates are found by orbital remote sensing and surface exploration missions. References ((red star = orbital observation; blue star = landed mission observation): 1. *Ackiss and Wray* [2014]; 2. *Arvidson et al.* [2005]; 3. *Arvidson et al.* [2010]; 4. *Bibring et al.* [2006]; 5. *Bibring et al.* [2007]; 6. *Bishop et al.* [2009]; 7. *Carter et al.* [2010]; 8. *Catling et al.* [2006]; 9. *Clark and Van Hart* [1981]; 10. *Dobrea et al.* [2008]; 11. *Farrand et al.* [2009]; 12. *Fishbaugh and Head* [2005]; 13. *Fishbaugh et al.* [2007]; 14. *Flahaut et al.* [2010]; 15. *Gendrin et al.* [2005]; 16. *Haskin et al.* [2005]; 17. *Horgan et al.* [2009]; 18. *Kounaves et al.* [2010]; 19. *Langevin et al.* [2005]; 20. *Lichtenberg et al.* [2010]; 21. *Liu et al.* [2012]; 22. Y. Liu et al. (in revision, 2015); 23. *Mangold et al.* [2007]; 24. *Mangold et al.* [2008]; 25. *Massé et al.* [2008]; 26. *McLennan et al.* [2013]; 27. *McSween et al.* [1999]; 28. *Milliken et al.* [2008]; 29. *Murchie et al.* [2009]; 30. *Roach et al.* [2009]; 31. *Roach et al.* [2010]; 32. *Squyres et al.* [2004]; 33. *Swayze et al.* [2008]; 34. *Wang et al.* [2006a]; 35. *Weitz et al.* [2012]; 36. *Wendt et al.* [2011]; 37. *Wiseman et al.* [2010]; 38. *Wray et al.* [2009]; 39. *Wray et al.* [2010]; 40. *Wray et al.* [2011]; 41. *Vaniman et al.* [2013]).

observed in north polar regions [*Langevin et al.*, 2005; *Fishbaugh and Head*, 2005; *Fishbaugh et al.*, 2007; *Horgan et al.*, 2009], whereas other findings of Ca sulfates have localized distributions [*Wray et al.*, 2010; *Ackiss and Wray*, 2014]. In many of these reports, Fe and Ca sulfates have been reported to coexist with monohydrated and polyhydrated sulfates [*Bishop et al.*, 2009; *Lichtenberg et al.*, 2010; *Weitz et al.*, 2012; *Wray et al.*, 2011; *Ackiss and Wray*, 2014].

In comparison with the orbital remote sensing of surface exposures of sulfates on a global scale, the in situ measurements made during surface exploration missions (Vikings, Pathfinder, MER, Phoenix, and MSL) have revealed the existence of Mg, Ca, and Fe^{3+} sulfates at all landing sites, either in outcrop or within the subsurface regolith [*Arvidson et al.*, 2010; *Bish et al.*, 2013; *Blake et al.*, 2013; *Clark and Van Hart*, 1981; *Haskin et al.*, 2005; *Kounaves et al.*, 2010; *McLennan et al.*, 2013; *McSween et al.*, 1999; *Squyres et al.*, 2004; *Wang et al.*, 2006a; *Vaniman et al.*, 2013]. The surface expression of hydrous sulfates at some of the landing sites was either ambiguous or not found by orbital remote sensing (e.g., in Gusev Crater).

The second important phenomenon is the frequent coexistence of monohydrated sulfate layers and polyhydrated sulfate layers on Mars. This coexistence is observed at almost all locations where hydrous sulfates have been identified by remote sensing. At some locations, six to nine alternating layers of these two types of sulfates, known as interbedded sulfate stratigraphy (Figure 2 and Figure S1 in the supporting information) have been reported [*Roach et al.*, 2009; (Y. Liu et al., Spectral and stratigraphic mapping of hydrated minerals associated with interior layered deposits near the southern wall of Melas Chasma, in revision, *Journal of Geophysical Research*, 2015)]. At other locations, various stratigraphic sequences of the two, in some cases mixed with other sulfates and nonsulfates, have been observed [*Ackiss and Wray*, 2014; *Bishop et al.*, 2009; *Catling et al.*, 2006; *Dobrea et al.*, 2008; *Ehlmann et al.*, 2009; *Flahaut et al.*, 2010; *Lichtenberg et al.*, 2010; *Liu et al.*, 2012; *Massé et al.*, 2008; *Mangold et al.*, 2007, 2008; *Murchie et al.*, 2009; *Roach et al.*, 2010; *Weitz et al.*, 2012; *Wendt et al.*, 2011; *Wiseman et al.*, 2010].

A key question regarding the frequent coexistence of the two most common and abundant hydrous sulfates on Mars relates to how the two hydrous sulfates with very different hydration degrees can coexist in a hyper-arid environment, i.e., in direct contact with the current Mars surface atmosphere. In other words, why did the

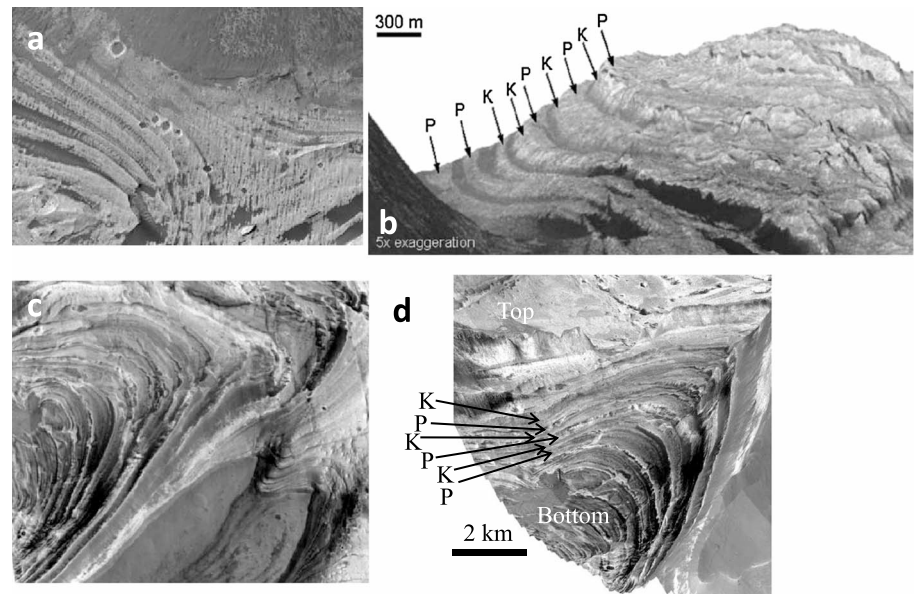


Figure 2. Interbedded sulfate stratigraphy seen on Mars. K = kieserite, P = polyhydrated sulfates. (a, b) East Chondor Chasma [Roach *et al.*, 2009]; (c, d) South Melas Chasma (Y. Liu *et al.*, in revision, 2015).

dehydration process of some sulfates stop in one layer at a polyhydrated stage but progress in the next layer to reach a monohydrated stage?

The goal of this study is to establish constraints on the nature, origin, and coexistence of monohydrated and polyhydrated sulfates, using knowledge gained from laboratory experimental studies, in combination with analyses of subsurface salts from a saline playa (Dalangtan, DLT) in a terrestrial hyperarid region (Qaidam basin, Tibet Plateau) (Wang *et al.*, submitted manuscript, 2015).

2. Basis of Experimental Design

2.1. Nature of Polyhydrated Sulfates: Current Knowledge

Martian sedimentary minerals are found to be rich in Mg and Fe, moderate in Ca, and poor in Na and K [McLennan, 2012a, 2012b]. This compositional feature is a reflection of a lower alteration degree on Mars (than that on Earth), and a higher dissolution rate of olivine than those of pyroxene, plagioclase, and K-feldspar [Hurowitz *et al.*, 2006; McLennan, 2012a, 2012b]. On this basis, we would anticipate the types of cations in Martian sulfates to have a descending abundance as follows: Mg, Fe, Ca, to Al, Na, K. A potential disruption of this order of abundance could come from cations released from volcanic glasses, which are relatively easier to alter or weather than feldspar and which can release Mg, Fe, Ca, Al, and other cations [Nesbitt and Wilson, 1992].

With the cation abundance order for sulfate formation on Mars in mind, we compared the Vis-NIR reflectance spectra of Mg, Fe²⁺, Fe³⁺, Ca, Al, Na, and K sulfates taken in the laboratory [Kong *et al.*, 2011; Ling and Wang, 2010; Liu and Wang, 2015; Wang and Zhou, 2014; McCollum *et al.*, 2014; Wang *et al.*, 2009; Wray *et al.*, 2010] (see also Figure S2) with typical OMEGA and CRISM spectra of polyhydrated sulfate (Figure 3). On the basis of their Vis-NIR spectral features, Fe³⁺, Ca, Al, Na, and K sulfates were excluded from the list of candidates that might contribute to the spectral features of polyhydrated sulfate.

Among the remaining candidates (Mg and Fe²⁺ sulfates) for polyhydrated sulfate, those with high degrees of hydration, i.e., MgSO₄·xH₂O (where x = 11, 7, and 6) and FeSO₄·xH₂O (where x = 7 or 6), can also be excluded for the following two reasons: (1) OMEGA or CRISM instruments sense only the top ~1 mm thick layer of Martian materials that are in equilibrium with the current hyperarid Martian atmosphere, (2) laboratory experiments on the stability field of Mg and Fe sulfates suggest that the species with high degrees (6–11 structural H₂O) of hydration in these two series would quickly dehydrate, within minutes or hours, at the

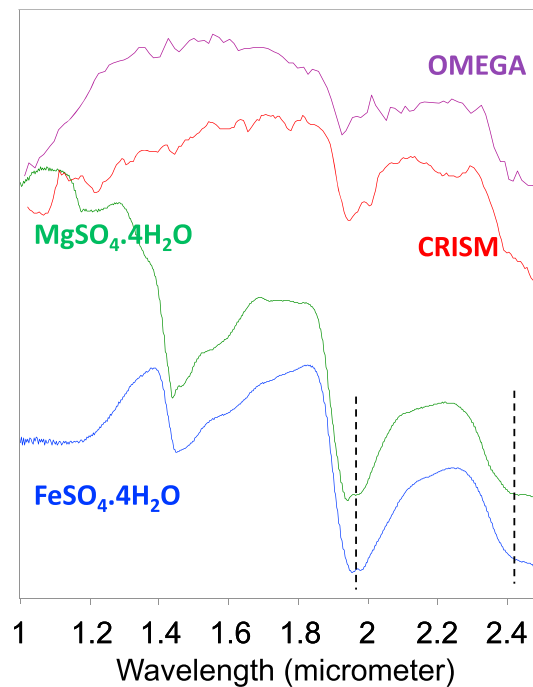


Figure 3. Two typical OMEGA and CRISM spectra of polyhydrated sulfate (OMEGA data #308 and CRISM data FRT00013F5B from Melas Chasma region on Mars), compared with the diffuse reflectance spectra of synthesized starkeyite $\text{MgSO}_4 \cdot 4\text{H}_2\text{O}$ and rozenite $\text{FeSO}_4 \cdot 4\text{H}_2\text{O}$.

range [Wang *et al.*, 2006b, 2009, 2011], we found that the dehydration of $\text{MgSO}_4 \cdot x\text{H}_2\text{O}$ ($x = 11, 7, \text{ and } 6$) at $T \leq 50^\circ\text{C}$ stops at the stage of starkeyite, $\text{MgSO}_4 \cdot 4\text{H}_2\text{O}$, with no further dehydration to monohydrate $\text{MgSO}_4 \cdot \text{H}_2\text{O}$, except under two specific circumstances [Wang *et al.*, 2009] that are presented in section 4.1. The upper temperature limit of 50°C for these simulation experiments was chosen on the basis of the surface temperature measured by recent missions on Mars and the fact that Mars climate models do not support a temperature $>50^\circ\text{C}$ at the surface at any time in Martian history [Smith *et al.*, 2004, 2006; Spanovich *et al.*, 2006; Harri *et al.*, 2014].

In order to constrain the nature of polyhydrated sulfate on Mars, we need to study the dehydration process of $\text{FeSO}_4 \cdot x\text{H}_2\text{O}$ ($x = 7 \text{ and } 6$) at $T \leq 50^\circ\text{C}$ (section 3.1), and to compare the results with those of $\text{MgSO}_4 \cdot x\text{H}_2\text{O}$ ($x = 11, 7, \text{ and } 6$).

2.2. Origin of Monohydrated Mg Sulfate: Past Experiments and Two Schools of Thought

Experiments on thermodynamic properties of Mg sulfates $\text{MgSO}_4 \cdot x\text{H}_2\text{O}$ ($x = 11 \text{ to } 0$) have demonstrated that at $T \geq 69^\circ\text{C}$, kieserite $\text{MgSO}_4 \cdot \text{H}_2\text{O}$ would directly precipitate from $\text{Mg-SO}_4\text{-H}_2\text{O}$ brine [van't Hoff *et al.*, 1912; Chou and Seal, 2007]. We anticipate that this high- T precipitation could occur during hydrothermal or volcanic events on Mars, when $\text{Mg-SO}_4\text{-H}_2\text{O}$ brine was available and the temperature exceeded 69°C . Nevertheless, high- T kieserite precipitation can explain neither the wide distribution of Martian $\text{MgSO}_4 \cdot \text{H}_2\text{O}$ at various geomorphologic sites nor its coexistence with polyhydrated sulfate that would precipitate at lower temperatures. Therefore, we need to find a pathway that can explain the formation of the majority of observed Martian $\text{MgSO}_4 \cdot \text{H}_2\text{O}$ at relative low temperatures, e.g., $\leq 50^\circ\text{C}$.

There are two schools of thought on the low- T formation of Mg sulfate monohydrate: (1) by dehydration or (2) by direct precipitation. The first school of thought is based on dehydration-rehydration experiments at $T \leq 50^\circ\text{C}$ in a wide range of relative humidity (RH) including vacuum desiccation in which $P_{\text{H}_2\text{O}}$ was maintained in a Martian $P_{\text{H}_2\text{O}}$ range [Chipera and Vaniman, 2007; Wang *et al.*, 2006b, 2009, 2011; Vaniman *et al.*, 2004; Vaniman and Chipera, 2006]. These studies suggest that Martian $\text{MgSO}_4 \cdot \text{H}_2\text{O}$ is the dehydration product

Martian surface under current Martian atmospheric conditions [Chipera and Vaniman, 2007; Wang *et al.*, 2006b, 2009, 2011; Wang and Zhou, 2014; Wang and Connor, 2014; Vaniman and Chipera, 2006].

The remaining potential candidates for polyhydrated sulfate are starkeyite, $\text{MgSO}_4 \cdot 4\text{H}_2\text{O}$, and rozenite, $\text{FeSO}_4 \cdot 4\text{H}_2\text{O}$. These minerals have almost indistinguishable NIR spectral features when compared with the typical (low signal-to-noise ratio) OMEGA and CRISM spectra of polyhydrated sulfate obtained from Mars (Figure 3). These two sulfates have intermediate degrees of hydration and were found in dehydration products of Mg and Fe sulfates with high degrees of hydration [Wang *et al.*, 2009; Wang and Connor, 2014]. Other Mg sulfates with intermediate hydration degree ($\text{MgSO}_4 \cdot x\text{H}_2\text{O}$, where $x = 5, 3, \text{ and } 2$) are extremely rare in terrestrial occurrences and have been found to be unstable in the laboratory [Chou and Seal, 2003, 2007; Wang *et al.*, 2006b]. Fe sulfates other than $\text{FeSO}_4 \cdot x\text{H}_2\text{O}$ (where $x = 7, 6, 4, \text{ and } 1$) do not occur naturally on Earth, and we infer that they also are unlikely to occur on Mars.

In three early sets of experiments, at temperatures (T) = 50°C , 21°C , 5°C , -10°C , and 10 different relative humidity (RH) levels in the 6–100%

Table 1. Temperature (°C) and Relative Humidity (RH in %) Conditions Used in 90 Experiments on $\text{FeSO}_4 \cdot x\text{H}_2\text{O}$ ($x = 7, 4, 1$)

RH Buffer Salts	5°C	21°C	50°C
LiBr	7%	7%	6%
LiCl	11%	11%	11%
MgCl ₂	34%	33%	31%
Mg(NO ₃) ₂	59%	54%	45%
NaBr	64%	59%	51%
KI	73%	70%	64%
NaCl	76%	75%	74%
KCl	88%	85%	81%
KNO ₃	96%	94%	85%
H ₂ O	100%	100%	100%

from Mg sulfates with high degrees of hydration (i.e., meridianiite, epsomite, and hexahydrite, with 11–6 structural H₂O molecules per formula unit) through two specific pathways (section 4.1). The second school of thought is based on geochemical modeling calculations (using the Pitzer model) on the precipitation sequence of a brine system with high ionic strength at $T \sim 25^\circ\text{C}$. The model calculations [Catalano *et al.*, 2012; Liu *et al.*, 2002] suggest that with sufficiently high ionic strength in

Cl-enriched Mg-SO₄-Cl-H₂O brine (Cl:SO₄ mole ratio ≥ 4.5 was used in Liu *et al.* [2002]), the water activity of the brine would be reduced to a level that would support the direct precipitation of kieserite, instead of the precipitations of epsomite or hexahydrite.

In order to understand the origin of the majority of Martian MgSO₄·H₂O, we need to study the precipitation of Mg sulfates from Cl-enriched Mg-SO₄-Cl-H₂O brines experimentally (section 3.2) to test or validate the above model predictions.

Monohydrated Mg sulfate MgSO₄·H₂O has two polymorphs, observed by both Chipera and Vaniman [2007] and Wang *et al.* [2009] in experiments. They were studied in detail using synthesis, X-ray diffraction (XRD), Raman, Mid-IR spectroscopy by Wang *et al.* [2009] and designated as LH-1w (i.e., MgSO₄·H₂O formed at low humidity levels, i.e., $\leq 33\%$ RH) and kieserite natural or laboratory formed MH-1w (i.e., MgSO₄·H₂O formed at mid humidity levels, i.e., $\geq 51\%$ RH). These two polymorphs have slightly different XRD patterns [Chipera and Vaniman, 2007; Wang *et al.*, 2009, Figure 13] but highly distinct Raman and Mid-IR spectra [Wang *et al.*, 2009, Figures 14 and 15]. Gravimetric measurements before and after baking at 400°C confirmed that both polymorphs have one structural H₂O per MgSO₄ formula unit.

More importantly, the two polymorphs LH-1w and kieserite (or MH-1w) form through different paths. LH-1w has been observed as the end product of dehydration of MgSO₄· x H₂O ($x = 11$ to 4) by Chipera and Vaniman [2007] and by Wang *et al.* [2009]. MH-1w, with an XRD pattern similar to that of natural kieserite (e.g., from Lehrte, Germany), only formed at middle to high RH conditions, either directly precipitated from aqueous brines of Mg-SO₄-H₂O at high T (e.g., at $T > 95^\circ\text{C}$ reported by Wang *et al.* [2009], with relevance for hydrothermal processes) or converted slowly from LH-1w at intermediate level RH (51%) and higher T (50°C) [Wang *et al.*, 2009].

3. Experiments, Observations, and Interpretations

Two new sets of experiments were designed and conducted to address the needs stated in sections 2.1 and 2.2.

3.1. Dehydration of FeSO₄·7H₂O—To Understand the Nature of Polyhydrated Sulfate

3.1.1. Samples and Experiments

We conducted 90 experiments on dehydration, rehydration, and deliquescence of three ferrous sulfates at three temperatures ($T = 50^\circ\text{C}$, 21°C , and 5°C) and 10 relative humidity levels (in the 6–100% range, Table 1). Pure chemicals, melanterite (FeSO₄·7H₂O), rozenite (FeSO₄·4H₂O), and szomolnokite (FeSO₄·H₂O), were used as starting phases. Sample identifications were made by XRD and laser Raman spectroscopy (based on the standard Raman spectra published by Chio *et al.* [2007]). Sample homogeneity in degree of hydration was confirmed by 100 spot checks using laser Raman spectroscopy on each of the starting samples. For each experiment, the starting sample (about 50 mg, 90–150 μm grain size) was placed in a reaction vial (~10 mm diameter and 40 mm height). The unsealed reaction vial was placed into a glass bottle (~25 mm diameter and 50 mm height) half-filled with an RH buffer solution [Chou and Seal, 2003; Greenspan, 1977]. Ten RH buffer solutions were used. Ten pairs of reaction vials and RH buffer bottles were then placed in an environment with controlled temperature, i.e., $50 \pm 1^\circ\text{C}$ in an oven, $21 \pm 1^\circ\text{C}$ on laboratory bench top, and $5 \pm 1^\circ\text{C}$

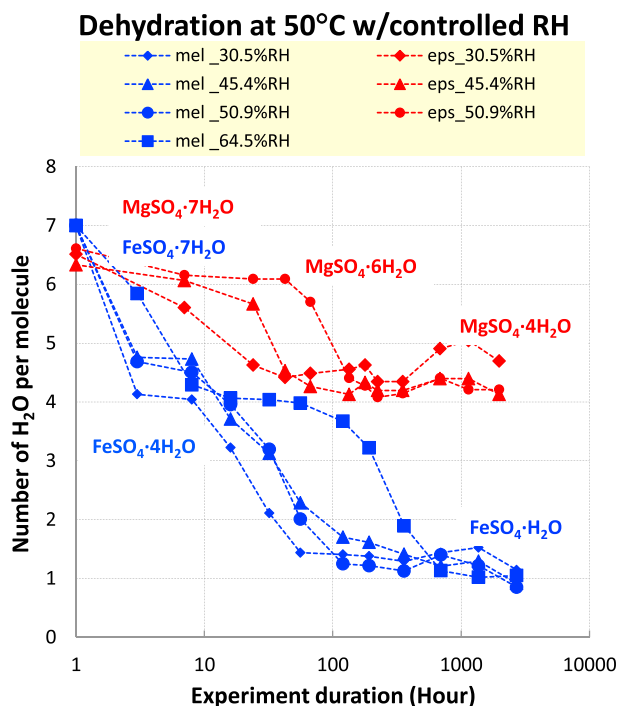


Figure 4. Comparison of dehydration pathways and end products of epsomite $\text{MgSO}_4 \cdot 7\text{H}_2\text{O}$ and melanterite $\text{FeSO}_4 \cdot 7\text{H}_2\text{O}$ at 50°C with controlled relative humidity (RH). The dehydration of $\text{FeSO}_4 \cdot 7\text{H}_2\text{O}$ reached $\text{FeSO}_4 \cdot \text{H}_2\text{O}$ while $\text{MgSO}_4 \cdot 4\text{H}_2\text{O}$ remained. This phenomenon demonstrates the lower stability of Fe sulfate(s) than Mg sulfate(s) against dehydration. Phase identifications were made using laser Raman spectroscopy.

in a refrigerator, thus 30 experiments for each of the three ferrous sulfates: melanterite, rozenite, and szomolnokite. These 90 sets of T -RH-driven experiments on dehydration, rehydration, and deliquescence of three ferrous sulfates lasted over 21 months, and 88 have reached equilibrium at the time of this manuscript writing. The reaction products were measured at intervals of 3, 8, and 16 h and 1.3, 2.3, 5, 8, 15, 29, 57, 113, 203, 327, and 483 days, at 14 intermediate stages of the experiments. At each intermediate stage, the reaction vial was removed from the RH buffer bottle, sealed immediately, and then we made noninvasive gravimetric and laser Raman spectroscopic measurements. We used gravimetric measurements to extract the average loss or gain in H_2O per Fe sulfate molecule from its starting degree of hydration. We used laser Raman spectroscopic measurements to make molecular phase identifications. These Raman measurements were made with the excitation laser beam passing through—and Raman photons collected through—the transparent glass wall of the sealed reaction vial. A low laser power density (3 mW of 532 nm continuous wave line with a $6\ \mu\text{m}$ beam diameter) was used. For each sample at every intermediate stage, at least three sampling spots were checked by Raman spectroscopy to determine the homogeneity of reaction products. Attainment of equilibrium of a dehydration-rehydration experiment is marked by (1) no more mass change in gravimetric measurement and (2) no more change in phase identifications in repeated Raman measurements.

3.1.2. Observations From Experiments

Through 30 dehydration experiments on melanterite ($\text{FeSO}_4 \cdot 7\text{H}_2\text{O}$), we found a reaction rate and final products that were very different from similar dehydration experiments on epsomite ($\text{MgSO}_4 \cdot 7\text{H}_2\text{O}$) (Figure 4). At 50°C and middle to low RH levels (65%, 51%, 45%, and 31%), the dehydration of melanterite $\text{FeSO}_4 \cdot 7\text{H}_2\text{O}$ reached the szomolnokite $\text{FeSO}_4 \cdot \text{H}_2\text{O}$ stage in 56 h (at 30.5% RH) to 360 h (at 64.5% RH). The Raman spectra of three ferrous sulfates shown in Figure S3 indicate that the phase identification of products is straightforward. In comparison, under the same conditions, the dehydration of epsomite $\text{MgSO}_4 \cdot 7\text{H}_2\text{O}$ at 50°C stopped at the starkeyite $\text{MgSO}_4 \cdot 4\text{H}_2\text{O}$ stage and never reached the monohydrated $\text{MgSO}_4 \cdot \text{H}_2\text{O}$ stage (Figure 4, with Raman spectra shown in Figure S4), except through two specific pathways (to be discussed in section 4.1). A similar dehydration rate comparison based on experiments at 21°C and 5°C also demonstrate the lower stability of Fe sulfates compared to Mg sulfates against dehydration (Figure S4).

3.1.3. Structural Reasons for Metastability of Starkeyite and Lower Stability of Rozenite in Dehydration at $T \leq 50^\circ\text{C}$

The metastability of substructural units in starkeyite ($\text{MgSO}_4 \cdot 4\text{H}_2\text{O}$) during dehydration at $T \leq 50^\circ\text{C}$ likely prevents the formation of $\text{MgSO}_4 \cdot \text{H}_2\text{O}$, based on the following reasons. The key substructural unit in the starkeyite structure is the four-member ring [Baur, 1964] made of two $[\text{SO}_4]$ tetrahedra and two $[\text{MgO}_2(\text{H}_2\text{O})_4]$ octahedra sharing corner oxygen atoms (Figure 5a). In comparison, the kieserite structure [Bregeault et al., 1970; Hawthorne et al., 1987] has a tightly interconnected 3-D framework made by sharing all coordinating oxygen atoms of an $[\text{SO}_4]$ tetrahedron with four Mg centered octahedra (Figure 5b). The large structural difference between starkeyite and kieserite requires additional activation energy to first break down the

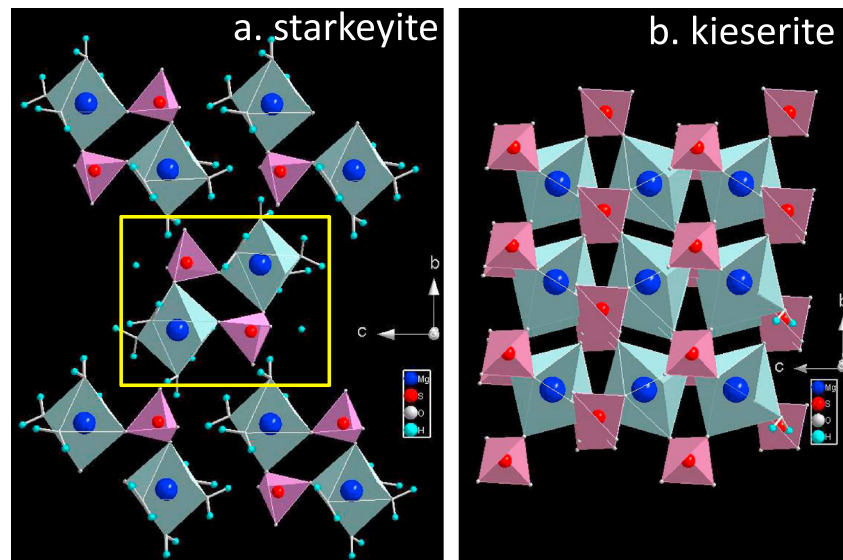


Figure 5. Structures of (a) starkeyite $\text{MgSO}_4 \cdot 4\text{H}_2\text{O}$ and (b) kieserite $\text{MgSO}_4 \cdot \text{H}_2\text{O}$. A four-member-ring substructural unit in starkeyite is enclosed by a yellow rectangle.

four-member rings in starkeyite and then to reorganize the octahedra and tetrahedra into a compact kieserite structure (the density of starkeyite and kieserite are 2.01 and 2.57 g/cm^3 , respectively). Apparently, a temperatures range $\leq 50^\circ\text{C}$ does not provide enough energy to overcome the large structural difference of starkeyite and kieserite, resulting in the metastability of starkeyite at $T \leq 50^\circ\text{C}$.

Rozenite $\text{FeSO}_4 \cdot 4\text{H}_2\text{O}$ has a similar substructural unit [Baur, 1962], the four-member ring made of two $[\text{SO}_4]$ tetrahedra and two $[\text{FeO}_2(\text{H}_2\text{O})_4]$ octahedra (a structure very similar to Figure 5a but replace Mg^{2+} by Fe^{2+}); however, rozenite has a slightly larger ring size, caused by a slightly larger $[\text{FeO}_2(\text{H}_2\text{O})_4]$ octahedron. Comparing the average bond length (2.076 Å) in $[\text{MgO}_2(\text{H}_2\text{O})_4]$ octahedra and the average S–O bond length (1.472 Å) in $[\text{SO}_4]$ tetrahedra in starkeyite, the lengths of same types of bonds in rozenite are 2.103 Å and 1.491 Å, respectively. The larger $[\text{FeO}_2(\text{H}_2\text{O})_4]$ octahedra and $[\text{SO}_4]$ tetrahedra in rozenite generate a larger four-member ring with an average S–Fe distance of 3.275 Å, whereas the average S–Mg distance in starkeyite is 3.245 Å. We infer that the larger $[\text{FeO}_2(\text{H}_2\text{O})_4]$ octahedron in rozenite would be less capable of holding its coordinating H_2O as tightly as is the case for $[\text{MgO}_2(\text{H}_2\text{O})_4]$ in starkeyite, which makes rozenite less resistant to dehydration. Our experiments show that under the same conditions at $T \leq 50^\circ\text{C}$, the dehydration of melanterite passes over the rozenite stage and reaches the monohydrated stage, szomolnokite $\text{FeSO}_4 \cdot \text{H}_2\text{O}$ (Figure 4).

We observed a similar instability for another Fe centered octahedron when compared with a Mg centered octahedron. During the dehydration of melanterite (Figure 4), a direct phase transition from $\text{FeSO}_4 \cdot 7\text{H}_2\text{O}$ to $\text{FeSO}_4 \cdot 4\text{H}_2\text{O}$ occurred in < 10 h, whereas the dehydration of epsomite under the same experimental conditions results in a stable presence of hexahydrate $\text{MgSO}_4 \cdot 6\text{H}_2\text{O}$, over 100 h at 51% RH (Figure 4). This phenomenon demonstrates the lower stability of $[\text{Fe}(\text{H}_2\text{O})_6]$ in $\text{FeSO}_4 \cdot 6\text{H}_2\text{O}$ compared to $[\text{Mg}(\text{H}_2\text{O})_6]$ in $\text{MgSO}_4 \cdot 6\text{H}_2\text{O}$.

The lower stability of rozenite revealed through the dehydration of melanterite at $T \leq 50^\circ\text{C}$ suggests a constraint, i.e., rozenite should not be stable at the present-day Martian surface and therefore does not contribute the vis-NIR spectral features of polyhydrated sulfate. In other words, when epsomite and melanterite both formed on Mars through weathering of basaltic minerals and by precipitation from the Mg-Fe-SO₄-H₂O system, their dehydration products in the general Martian surface T range (i.e., not during hydrothermal or volcanic events with much higher T) would have been starkeyite ($\text{MgSO}_4 \cdot 4\text{H}_2\text{O}$) and szomolnokite ($\text{FeSO}_4 \cdot \text{H}_2\text{O}$). Starkeyite would remain metastable on Mars unless involved in two other processes (discussed below, in section 4.1) and would contribute spectral features similar to those assigned to polyhydrated sulfate on the basis of OMEGA and CRISM data. Szomolnokite would either contribute spectral features with slightly shifted band centers from those of

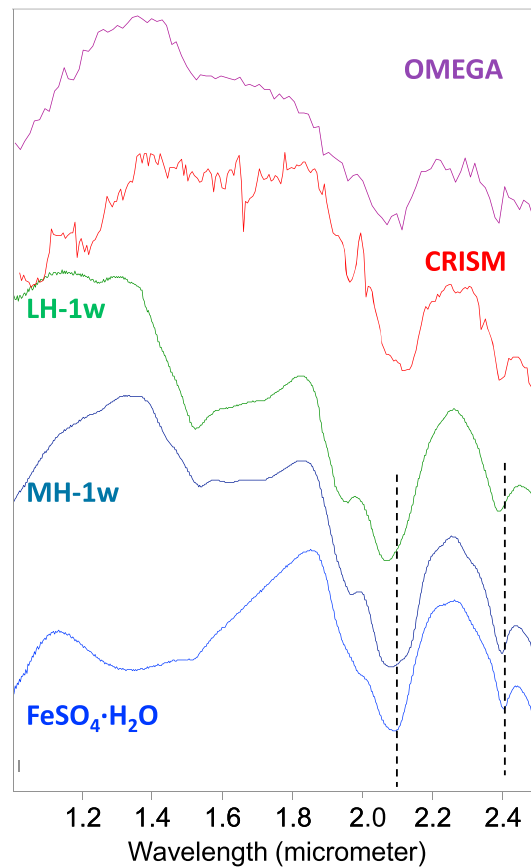


Figure 6. Laboratory spectra of monohydrated Mg sulfates (LH-1w and MH-1w) and $\text{FeSO}_4 \cdot \text{H}_2\text{O}$ (szomolnokite), compared with OMEGA and CRISM monohydrated Mg sulfate spectrum (OMEGA data #308 and CRISM data FRT00013F5B from Melas Chasma region on Mars).

precipitated crystals themselves. Because the solubility of MgCl_2 (56 g per 100 g H_2O at 25°C [Lide, 2001]) is much higher than that of MgSO_4 (36 g per 100 g H_2O), bischofite $\text{MgCl}_2 \cdot 6\text{H}_2\text{O}$ would precipitate later in the process, which was confirmed by repeated in situ Raman measurements of the precipitated crystals through the evaporation-precipitation process. Therefore, the local RH during Mg sulfate precipitation for eight brine samples was mainly controlled by $\text{MgCl}_2 \cdot \text{H}_2\text{O}$ saturated solutions (33.0–33.6% RH at 21°C and 5°C, based on Greenspan [1977]). Furthermore, we placed the two brine samples with the highest Cl content ($\text{Cl}:\text{SO}_4 = 18:1$) at lower RH, into two desiccators whose RH levels were buffered by a $\text{LiCl} \cdot \text{H}_2\text{O}$ saturated solution (RH = 11.3% at 21°C and 5°C). In this way, their evaporation-precipitation processes were forced to take place in an environment with much lower water activity than can be maintained by saturated $\text{Mg} \cdot \text{SO}_4 \cdot \text{Cl} \cdot \text{H}_2\text{O}$ brine to further verify the Pitzer model predictions [Catalano et al., 2012; Liu et al., 2002] at an extreme RH condition.

During the entire evaporation-precipitation process of 10 brine samples, repeated in situ Raman measurements were made directly on the precipitated crystals starting from day 2 (when early crystals formed) until full solidification of the entire brine. Then, repeated Raman spectroscopic monitoring on dry crystals was done until day 124 of the experiments.

The pseudonatural brine was generated by dissolving a natural salt-rich soil sample from a saline playa in a hyperarid region (Dalangtan (DLT) saline playa, Qaidam basin, on the Tibet Plateau), where the local aridity index is less than 0.04 (A. Wang et al., submitted manuscript, 2015), into small amounts of Millipore H_2O . The original sample has a $\text{Cl}:\text{SO}_4$ ratio of $\sim 7.8:1$ (i.e., 78 times that commonly observed on Mars) and was found to contain Na, Mg, Li, Ca, and K. The evaporation-precipitation process was maintained at 21°C and

$\text{MgSO}_4 \cdot \text{H}_2\text{O}$ (Figure 6) [Bishop et al., 2009; Weitz et al., 2012] or it would transform to Fe-bearing hydroxides and oxides through later processes [Tosca and McLennan, 2008].

3.2. Evaporation of $\text{Mg} \cdot \text{SO}_4 \cdot \text{Cl} \cdot \text{H}_2\text{O}$ Brines With High Ionic Strength—To Constrain the Origin of Martian Monohydrated Mg Sulfate

3.2.1. Samples and Experiments

In order to validate the model prediction [Catalano et al., 2012; Liu et al., 2002], we conducted two sets of evaporation-precipitation experiments of Cl rich $\text{Mg} \cdot \text{SO}_4 \cdot \text{Cl} \cdot \text{H}_2\text{O}$ brines; one set used synthetic brines and one set used a pseudonatural brine made from a natural salty soil sample.

The synthetic brine samples in the $\text{Mg} \cdot \text{SO}_4 \cdot \text{Cl} \cdot \text{H}_2\text{O}$ system were made by dissolving $\text{MgSO}_4 \cdot 7\text{H}_2\text{O}$ and $\text{MgCl}_2 \cdot 6\text{H}_2\text{O}$ into small amounts of Millipore H_2O . The commonly observed molar ratio in Martian samples is $\text{Cl}:\text{SO}_3 \sim 1:10$ [Clark et al., 2005; Gellert et al., 2006]. The $\text{Cl}:\text{SO}_4$ ratio of the starting brine in Liu et al. [2002] Pitzer modeling was 4.5 and higher. In order to test the extreme cases, we made the synthetic brine samples with $\text{Cl}:\text{SO}_4$ molar ratios of 2:9, 6:7, 10:5, 14:3, and 18:1, i.e., 4, 8, 20, 46, and 180 times the common $\text{Cl}:\text{SO}_3$ ratio on Mars. These brine samples were placed in open petri dishes and maintained at $T = 21 \pm 1^\circ\text{C}$ and $T = 5 \pm 1^\circ\text{C}$ for brine evaporation and salt precipitation.

For eight of the 10 synthetic brines, the environmental relative humidity (RH) level during evaporation-precipitation was maintained by the brines and pre-

Table 2. Hydration Degree of the Mg Sulfates in Precipitations From Synthetic Brines of Mg-SO₄-Cl-H₂O System, Identified by Laser Raman Spectroscopy (7w = MgSO₄·7H₂O, 6w = MgSO₄·6H₂O, 5w = MgSO₄·5H₂O, and 4w = MgSO₄·4H₂O)

T	21°C					5°C				
	11.30%	RH Maintained by Brine Itself				11.30%	RH Maintained by Brine Itself			
Cl:SO ₄ Ratios in Brine	18:1	14:3	10:5	6:7	2:9	18:1	14:3	10:5	6:7	2:9
Phase after full solidification	6w	6w	6w	6w	6w, 7w	7w	7w	6w	7w	6w
Phase at day 124	5w, 6w _{trace}	5w, 6w	5w	4w, 6w	4w, 5w, 6w	5w, 6w	6w, 5w	6w	7w	7w

11% RH (buffered by an LiCl-H₂O solution). Repeated in situ Raman measurements were taken until the brine reached full solidification.

3.2.2. Observations in Experiments

Only epsomite MgSO₄·7H₂O and hexahydrate MgSO₄·6H₂O were identified by in situ Raman measurements on precipitated crystals (Table 2) formed in all 10 synthetic brines at 21°C and 5°C, including the two brines with the highest Cl:SO₄ (18:1) and evaporated at 11% RH. Bischofite MgCl₂·6H₂O was identified in a later stage of precipitation. In other words, no monohydrated Mg sulfate (MgSO₄·H₂O) was observed as a direct precipitate from the brine samples with Cl/SO₄ ratios being 2–180 times that commonly observed on Mars.

After full solidification, the precipitated crystals were kept at the same T-RH conditions until day 124. The Raman spectra of final products show the presence of additional MgSO₄·5H₂O and MgSO₄·4H₂O phases (Table 2). However, no MgSO₄·H₂O formed with further dehydration (Table 2 and Figure 7). On the basis of early studies of dehydration processes of Mg sulfates [Chipera and Vaniman, 2007; Wang et al., 2006b, 2009, 2011], we conclude that MgSO₄·5H₂O and starkeyite MgSO₄·4H₂O are the dehydration products of originally precipitated epsomite and/or hexahydrate in the T range used in these experiments.

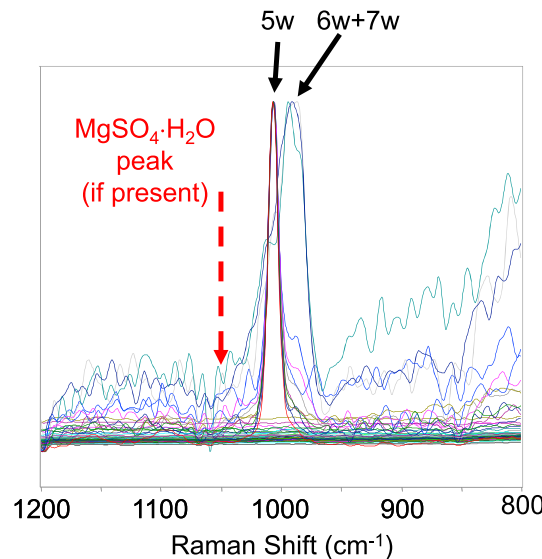


Figure 7. Raman spectra from 100 spots on the crystals precipitated from a synthetic brine of Mg-SO₄-Cl-H₂O system, with the highest Cl/SO₄ ratio in the experimental set (i.e., 180 times that commonly seen on Mars), after full solidification and until Day 124. MgSO₄·H₂O peak (1042–1046 cm⁻¹, Figure 9) is absent in all Raman scans of precipitates at intermediate and final stages of the experiments. The Raman peak positions in this plot indicate epsomite (7w, 984 cm⁻¹), hexahydrate (6w, 983 cm⁻¹), and MgSO₄·5H₂O (5w, 1005 cm⁻¹). MgCl₂·6H₂O is detected in the precipitation by its major Raman peaks at 3508, 3387, and 3354 cm⁻¹ (not shown in this plot).

From the evaporation-precipitation of the pseudonatural brine that belongs to the Na-Mg-Li-Ca-K-SO₄-Cl system, in situ Raman measurements indicate the presence of MgSO₄·7H₂O, MgSO₄·6H₂O, and CaSO₄·2H₂O in direct precipitation (Figure 8), with additional chloride hydrates KMgCl₃·6H₂O and halite NaCl (identified by XRD). Similar to the case of precipitation from synthetic brines, MgSO₄·H₂O was not found in the direct precipitation products from pseudonatural brine (Figure 8) or in the dehydration products.

These two experimental observations are validated by the characterization of hydration degrees of subsurface Mg sulfates in the DLT saline playa [Wang et al., 2014; A. Wang et al., submitted manuscript, 2015] (Figure S6). At this site, chlorides (mainly NaCl, with minor KCl) are widely distributed at the surface and within the subsurface. Carnallite (KMgCl₃·6H₂O), kainite (KCl·MgCl₂·3H₂O), polyhalite (K₂Ca₂Mg(SO₄)₄·2H₂O), and thenardite (Na₂SO₄) were found coprecipitated with Mg sulfates, which suggests extremely high ionic strength in the original brine. Among the abundant Mg sulfates in the subsurface, epsomite MgSO₄·7H₂O and hexahydrate MgSO₄·6H₂O are the major phases. MgSO₄·5H₂O and MgSO₄·4H₂O appear in some samples. No MgSO₄·H₂O was found in any subsurface salt

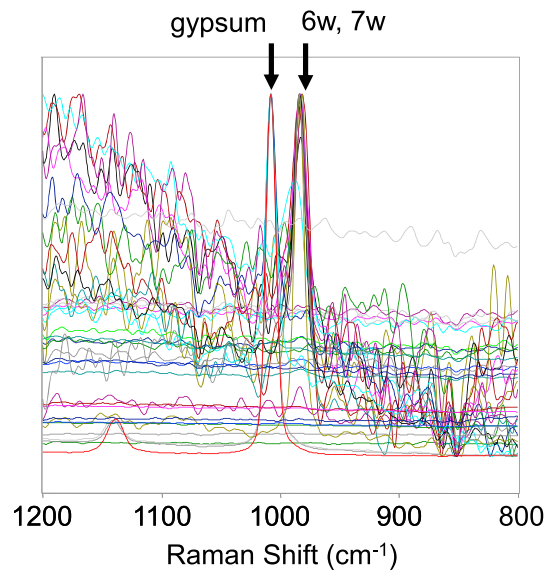


Figure 8. Raman spectra from 100 spots on the precipitated crystals from a pseudonatural brine in the Na-Mg-Li-Ca-K-SO₄-Cl-H₂O system, made from a natural salt sample collected from DaLangTan saline playa on Tibet Plateau. The brine has a Cl/SO₄ ratio of 7.8:1. After full solidification, the Raman peak positions indicate epsomite (7w), hexahydrate (6w), and gypsum CaSO₄·2H₂O (1008 cm⁻¹). The peak of MgSO₄·H₂O (1042–1046 cm⁻¹, Figure 9) is absent in all collected Raman spectra. KMgCl₂·6H₂O is present, with its major Raman peaks at 3428 cm⁻¹ (not shown in this plot). NaCl is also present and identified by XRD.

on the origin of the majority of Martian MgSO₄·H₂O, i.e., the results support the formation mechanism of MgSO₄·H₂O on Mars through dehydration. That is, the Mg sulfates with high degrees of hydration, MgSO₄·xH₂O (x = 11, 7, and 6) were likely the precursors of the majority of Martian MgSO₄·H₂O.

Among the two Mg sulfate monohydrate polymorphs, LH-1w and kieserite (MH-1w) described in section 2.2, the dehydration product would take the form of LH-1w. Thus, we anticipate that most Martian MgSO₄·H₂O at the surface would also take the form of LH-1w. The current T-RH conditions at the Martian surface would make the conversion from LH-1w to kieserite less likely to occur (because it would require an intermediate level RH, e.g., 51%). However, at locations where hydrothermal events could raise the local T > 69°C, the existence of kieserite by direct precipitation cannot be excluded.

4. Coexistence of MgSO₄·H₂O and MgSO₄·4H₂O on Mars

On the basis of two constraints established by the experiments described in section 3.1 and 3.2, and results from earlier reported experiments [Chipera and Vaniman, 2007; Wang et al., 2006b, 2009, 2011], we infer that starkeyite (MgSO₄·4H₂O) is the best candidate for polyhydrated sulfate on Mars (formed through the path indicated by blue colored arrows in Figure 10). We infer that the majority of Martian MgSO₄·H₂O (monohydrate) formed through the dehydration of Mg sulfates with higher degrees of hydration (i.e., MgSO₄·xH₂O, x = 11, 7, and 6) and that upon dehydration, it takes the form of LH-1w (formed through the path indicated by red colored arrows in Figure 10).

In light of these results, a relevant question is how two Mg sulfates with very different hydration degrees could coexist in a hyperarid environment, in direct contact with the current Martian surface atmosphere for millions of years? Why would the dehydration process of hydrous sulfates result in one layer with MgSO₄·4H₂O but progress in an adjacent layer to reach a monohydrated MgSO₄·H₂O stage? In addition, when were the observed hydration degrees set?

samples. On the other hand, after subsurface salts were exposed by local mining activities (Figure S6) and experienced direct interaction with the regional hyperarid atmosphere, monohydrated MgSO₄·H₂O (in the form of LH-1w) was identified at the surface of some samples (Figure 9); this observation is discussed below in section 4.1.

3.2.3. Inferences From Experimental Results

In the experiments described in section 3.2 (with Cl/SO₄ ratios up to 180 times that commonly observed on Mars), we have not found evidence to support direct precipitation of MgSO₄·H₂O from Cl-enriched Mg-SO₄-Cl-H₂O brines as suggested by geochemical model calculations [Catalano et al., 2012; Liu et al., 2002]. This fact, together with the almost constant Cl:SO₃ ratio (~1:10) found in Mars' surface materials by landed missions [Clark and Van Hart, 1981; McSween et al., 1999; Gellert et al., 2006; Kounaves et al., 2010; McLennan et al., 2013] and the huge amount of MgSO₄·H₂O at the Martian surface revealed by orbital remote sensing (Bibring et al. [2006], and many others), suggests that it is highly unlikely that the large amount of Martian MgSO₄·H₂O (i.e., the monohydrate) originated from direct precipitation of Cl-enriched Mg-SO₄-Cl-H₂O brines. These observations in simulation experiments and in terrestrial field observations set a constraint

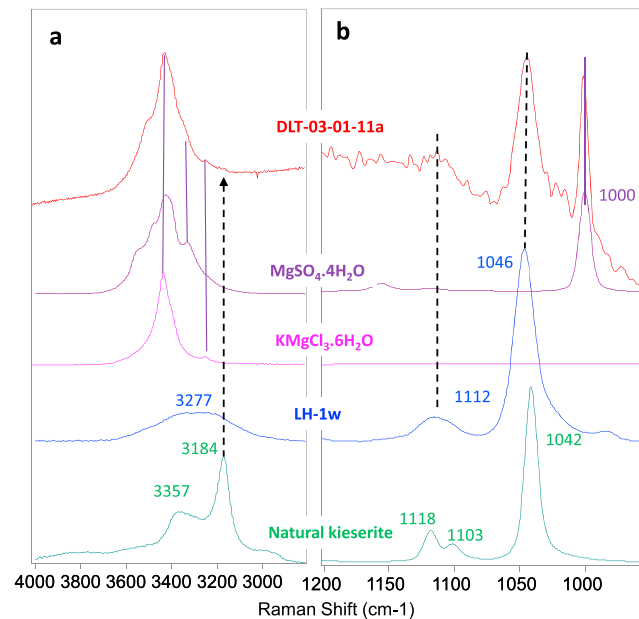


Figure 9. Raman spectrum of a sample collected from the Dalangtan saline playa (Tibet), DLT-03-01-11a. It is a subsurface soil sample partially exposed to surface atmospheric conditions. The Raman spectra of a natural kieserite from Lehrte (Germany), and laboratory synthesized LH-1w, starkeyite $\text{MgSO}_4 \cdot 4\text{H}_2\text{O}$, and carnallite $\text{KMgCl}_3 \cdot 6\text{H}_2\text{O}$ are shown for comparison: (a) $\text{H}_2\text{O}/\text{OH}$ vibration spectral range, (b) SO_4 fundamental vibration spectral range. The Raman spectral peak matching suggests that this sample contains mainly LH-1w. The evidence is as follows: in Figure 9b the matching of the two peaks with LH-1w is indicated by two black thick dotted lines, and in Figure 9a the absence of a sharp peak near 3184 cm^{-1} (one of the doublet of natural kieserite) is marked by a black thick dotted line. This sample also contains starkeyite and carnallite. The peak matching is indicated by four solid thin lines of purple color: in Figure 9b a peak matching with starkeyite main peak at 1000 cm^{-1} , and in Figure 9a the H_2O peaks of this sample matching with the combined H_2O peaks of starkeyite and carnallite (pink and purple spectra in Figure 9a). The H_2O peak of LH-1w has a large peak width and a low signal strength (blue spectrum in Figure 9a) that would be nondistinguishable when coexisting with the strong H_2O peaks of starkeyite and carnallite.

$\text{MgSO}_4 \cdot \text{H}_2\text{O}$ structure. The formation of $\text{MgSO}_4 \cdot \text{H}_2\text{O}$ in the form of LH-1w directly from amorphous Mg sulfates at $T \leq 50^\circ\text{C}$ has been demonstrated experimentally [Wang et al., 2009, Table 2 and 5].

The effect of *sudden exposure* of highly hydrated Mg sulfates to a hyperarid environment has been seen in samples from the DLT saline playa [Wang et al., 2014; A. Wang et al., submitted manuscript, 2015]. The local mining activities at DLT have excavated the subsurface Mg sulfates (originally with seven or six structural H_2O per MgSO_4 [Wang et al., 2014; A. Wang et al., submitted manuscript, 2015]) by making many large and deep trenches (Figure S6). The effects of hyperarid regional atmospheric condition (aridity index, $\text{AI} < 0.04$), would cause structural collapse of epsomite and hexahydrate and the formation of amorphous Mg sulfates. Under the local hyperarid conditions, the dehydration of amorphous Mg sulfates would continue and would form LH-1w at the surface of freshly exposed salts. The Raman spectrum of the DLT-03-01-11a sample in comparison with the spectra of kieserite, LH-1w, starkeyite, and carnallite, illustrates this phenomenon (Figure 9).

Pathway #2 is by catalysis (indicated by three red solid-line arrows in Figure 10). The experiments reported by Wang et al. [2009] revealed that the metastability of starkeyite can be overcome at relatively low temperature ($T \leq 50^\circ\text{C}$) by a catalysis effect. This finding was demonstrated through dehydration experiments of epsomite $\text{MgSO}_4 \cdot 7\text{H}_2\text{O}$ that was mixed separately with Ca sulfates (gypsum, basanite, and anhydrite) or with Fe^{2+} sulfate ($\text{FeSO}_4 \cdot 7\text{H}_2\text{O}$) and Fe^{3+} sulfates ($\text{Fe}_2(\text{SO}_4)_3 \cdot 7\text{H}_2\text{O}$ and $\text{Fe}_2(\text{SO}_4)_3 \cdot 5\text{H}_2\text{O}$), or with Fe_2O_3 and FeOOH .

4.1. Two Pathways of Forming LH-1w by Dehydration at $T \leq 50^\circ\text{C}$

To answer these questions, we examine the two phase transition pathways that have been found through some early experiments, which bypassed or helped to overcome the metastability of starkeyite at relatively low temperature ($T \leq 50^\circ\text{C}$) and then drove the progress of dehydration to the final stage to form $\text{MgSO}_4 \cdot \text{H}_2\text{O}$ in the form of LH-1w.

Pathway #1 is through an intermediate amorphization stage (indicated by two red dotted line arrows in Figure 10). The experiments reported by Vaniman et al. [2004], Vaniman and Chipera [2006], Wang et al. [2006b, section 4.5], and Wang et al. [2009, Table 2] revealed that amorphous Mg sulfates $\text{MgSO}_4 \cdot n\text{H}_2\text{O}$ ($n = 0.9$ to 3) would be formed when highly hydrated $\text{MgSO}_4 \cdot x\text{H}_2\text{O}$ ($x = 11, 7$, and 6) were suddenly exposed to a hyperarid environment. The formation of an amorphous phase at an intermediate stage can increase the rate of dehydration of the Mg sulfates. This pathway would bypass starkeyite as the middle stage of dehydration and thus would pose no requirement for excess activation energy to break down the four-member ring discussed above. In addition, the irregular structural framework of amorphous phases would be relatively easy to break, to reorganize, and to form the more compact

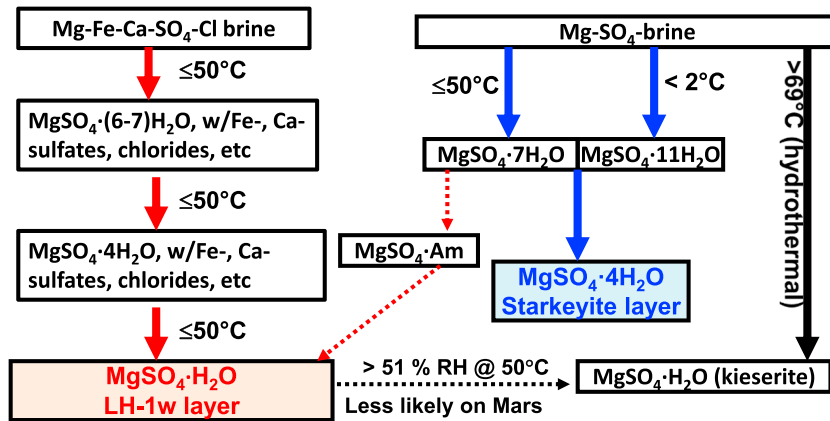


Figure 10. Pathways of Mg sulfate dehydrations that facilitate the formation of starkeyite, monohydrated Mg sulfates (LH-1w and kieserite), and the coexistence of LH-1w layers and starkeyite layers on Mars. The red solid arrows indicate the pathway of forming monohydrated Mg sulfate in the form of LH-1w from chemically complex brines. The blue solid arrows indicate that the dehydration of highly hydrated Mg sulfates from relatively pure Mg-SO₄ brines would stop at starkeyite at $T < 69^\circ\text{C}$. A black solid arrow indicates the precipitation of kieserite from brine at $T > 69^\circ\text{C}$. The red dotted arrows indicate a potential pathway of forming monohydrated Mg sulfate through the intermediate amorphous hydrous Mg sulfates. A black dotted arrow indicates a transition from LH-1w to the kieserite structure observed in the laboratory at $\text{RH} > 51\%$ and at 50°C .

MgSO₄·H₂O (LH-1w) was found to be the dehydration product in these mixing experiments (details in Tables 6 and 7 and evidence in Figures 11 and 12 of Wang *et al.* [2009]).

Recently, we completed a new set of dehydration experiments on epsomite that was mixed separately with NaCl, KCl, and KMgCl₃·6H₂O at 50°C and 11% and 33% RH. Table 3 lists the dehydration pathways in six subsets of mixing experiments, in comparison with the dehydration pathways of pure MgSO₄·7H₂O and FeSO₄·7H₂O under the same T -RH conditions. Phase identifications in all 10 subsets of experiments were made using Raman spectroscopy. Similar to the results in mixtures with Ca and Fe sulfates, and Fe oxides and oxyhydroxides [Wang *et al.*, 2009], MgSO₄·H₂O monohydrate was reached (in 5–118 days) during the dehydration of epsomite that was mixed with three chlorides (Table 3, with experimental details), while the dehydration of pure epsomite in a control experiment stopped at starkeyite MgSO₄·4H₂O (Table 3). Notably, formation of FeSO₄·H₂O (Fe1w in Table 3) occurred in one day at both RH levels, demonstrating the rapid dehydration rate of Fe sulfates, consistent with Figures 4 and S5. The results from these mixing experiments suggest that the microscopic local environments surrounding an epsomite grain maintained by the coexisting species (sulfates or chlorides, or Fe hydroxides or oxides) have helped the dehydration of epsomite to overcome the metastability of starkeyite and to form the monohydrate, MgSO₄·H₂O (LH-1w).

Table 3. Dehydration Pathways of MgSO₄·7H₂O^a

Day	MgSO ₄ 7H ₂ O Mixed w/NaCl		MgSO ₄ 7H ₂ O Mixed w/KCl		MgSO ₄ 7H ₂ O Mixed w/KMgCl ₃ ·6H ₂ O		Pure MgSO ₄ 7H ₂ O		Pure FeSO ₄ 7H ₂ O	
	11% RH	33% RH	11% RH	33% RH	11% RH	33% RH	11% RH	33% RH	11% RH	33% RH
1	4w, 6w	4w, 6w	6w, 4w	6w, 5w, 4w	4w, 5w	4w	4w, 6w	4w, 6w	Fe1w, Fe4w	Fe1w, Fe4w
2	4w, 6w	4w, 6w	4w, 6w	6w, 5w, 4w		4w	4w	4w	Fe1w, Fe4w	Fe1w, Fe4w
5	4w, 6w	4w, 6w	4w, 6w	4w, 6w	4w, 3w, 1w	4w	4w	4w	Fe1w	Fe1w
12	4w	4w, 6w	4w	4w, 5w, 6w	1w	4w	4w	4w	Fe1w	Fe1w
15	4w	4w, 6w	4w	4w, 6w	1w	4w	4w	4w	Fe1w	Fe1w
41	4w, 2w, 1w	4w, 6w	4w, 2w, 1w, 6w	4w, 3w, 1w	1w	1w	4w	4w	Fe1w	Fe1w
118	1w, 2w, 4w	1w, 4w, 6w	4w, 1w, 2w	2w, 3w, 4w	1w	1w, 6w	4w	4w	Fe1w	Fe1w

^aIt was mixed with NaCl, KCl, and KMgCl₃·6H₂O separately, at 1:9 molar ratio and maintained at 50°C in LiCl (11% RH) and MgCl₂ (33% RH) buffers. The dehydration pathways of mixtures are compared with those of pure MgSO₄·7H₂O and FeSO₄·7H₂O under the same T -RH conditions. The phase identifications were made by laser Raman spectroscopy. (6w, 5w, 4w, 3w, 2w, 1w = MgSO₄·xH₂O, where $x = 6, 5, 4, 3, 2, 1$; Fe1w, Fe4w = FeSO₄·yH₂O, where $y = 1, 4$; in boldface = the first appearance of 1w) or Fe1w; in italics = seeing MgCl₂·6H₂O from KMgCl₃·6H₂O decomposition).

Among the two pathways, we think the second pathway has the higher probability of occurring on Mars (red solid arrows in Figure 10). Chemically complex brines of the Mg-Fe-Ca-SO₄-Cl system can be readily generated from chemical weathering of basaltic rocks [McLennan, 2012a]. From those brines, MgSO₄·xH₂O (x = 11 or 7 or 6, depending on precipitation temperature) could precipitate together with other sulfates (Ca and Fe²⁺ sulfates) and chlorides. The coexistence of Ca, Fe²⁺ sulfates (and Fe³⁺ sulfates, Fe₂O₃, and FeOOH as possible alteration products from Fe²⁺ sulfates) would provide catalytic effects to overcome the metastability of starkeyite and thus facilitate the formation of MgSO₄·H₂O (LH-1w) at T ≤ 50°C (Figure 10).

On the other hand, we think that the first pathway (amorphization, red dotted arrows in Figure 10) has a lower likelihood of occurring during the diurnal cycle at the present-day Martian surface (as discussed in Wang *et al.* [2011]). However, at the vicinity of an impact crater, this pathway might generate some MgSO₄·H₂O in association with the sudden exposure of sulfate-bearing sediments by impact. Nevertheless, it cannot explain the broad coexistence of (or proximity of layers containing) the two Mg sulfates with different degrees of hydration.

4.2. Formation of Interbedded Stratigraphy and Other Sulfate Coexistence on Mars

Following the pathway discussion in section 4.1 (Figure 10), we hypothesize that (1) the dehydration of “dirty” Mg sulfates, i.e., those originally precipitated from a complex Mg-Ca-Fe-SO₄-Cl-H₂O brine, would progress to MgSO₄·H₂O (in the form of LH-1w) and thus form a LH-1w layer (solid red arrows in Figure 10); (2) the dehydration of “clean” Mg sulfates, i.e., those originally precipitated from a relatively pure Mg-SO₄-H₂O brine, would terminate at the stage of starkeyite (metastable at relatively low temperatures), thus forming a starkeyite layer (blue solid arrows in Figure 10).

There are two ways to generate the coexisting LH-1w layer and starkeyite layers on Mars. First, they could have been generated from unrelated episodic brines, with different chemistry. The chemistry and the quantity of the brine would be the determining factor for the resulting LH-1w layer or starkeyite layer and their thicknesses. The sequence of episodic brines input to a specific location would set the order of stratigraphic layers of hydrous sulfates at the location, i.e., sometimes LH-1w layer on top of starkeyite layer, or vice versa, as observed at most locations on Mars [Ackiss and Wray, 2014; Bishop *et al.*, 2009; Catling *et al.*, 2006; Dobrea *et al.*, 2008; Flahaut *et al.*, 2010; Lichtenberg *et al.*, 2010; Massé *et al.*, 2008; Mangold *et al.*, 2008; Murchie *et al.*, 2009; Roach *et al.*, 2010; Weitz *et al.*, 2012; Wiseman *et al.*, 2010; Wendt *et al.*, 2011].

Second, a pair of LH-1w and starkeyite layers could also result from two precipitation-dehydration stages from single complex Mg-Ca-Fe-SO₄-Cl-H₂O brine in the following way. The solubilities of CaSO₄ and FeSO₄ in water (0.205 and 29.5 g/100 g H₂O at 25°C [Lide, 2001]) are both lower than that of MgSO₄ (35.7 g/100 g H₂O at 25°C). From a Mg-Ca-Fe-SO₄-Cl-H₂O brine, the early precipitated sulfates would deplete the Ca and Fe cations in the brine, resulting in a late-stage brine that is relatively pure, as Mg-SO₄-H₂O. During the dehydration process of this two-stage sequence, the early precipitated Mg sulfates coexisting with catalytic species (Ca and Fe sulfates and chlorides) would dehydrate to MgSO₄·H₂O and form an LH-1w layer, whereas the dehydration of later-precipitated Mg sulfates from late-stage brine would terminate at a middegree of hydration and form a starkeyite layer. For interbedded sulfate stratigraphy of six to nine layers [Roach *et al.*, 2009; Y. Liu *et al.*, in revision, 2015], several input cycles of chemically complex brines would have to be involved, and each initial brine would have to experience two precipitation-dehydration stages that would generate one set of paired LH-1w and starkeyite layers.

Using this reasoning, we might be able to explain the formation of the upper three morphologic layers in Figure 2b (observed by Roach *et al.* [2009]), each has a “K-P” layer pair that follows the same order in all three morphologic layers, and similarly, the three “K-P” layer pairs in Figure 2d (observed by Y. Liu *et al.* (in revision, 2015)). These layers might form from three events of brine input. In the precipitation process from each brine, the LH-1w layer (called the K layer in Roach *et al.* [2009] and Y. Liu *et al.* (in revision, 2015)) in a “K-P” layer pair would be generated from the dehydration of the early “dirty” Mg sulfates precipitated from chemically complex brine and would form the base of a “K-P” layer pair. A starkeyite layer (called the P layer in Roach *et al.* [2009] and Y. Liu *et al.* (in revision, 2015)) would be generated from the dehydration of the later “clean” Mg sulfates precipitated from the remaining later-stage brine (depleted of Fe, Ca, etc.) and would be deposited at the top of the LH-1w base of the “K-P” layer pair. We suspect that both processes could have occurred on Mars, depending on the locations of sulfate deposits, local geochemistry, and geomorphology.

4.3. Effect of Obliquity Cycles

As discussed in section 4.2, we infer that the primary precipitation processes from episodic brine(s) would have established the chemical characteristics of deposited sulfate layers. During subsequent dehydration, these chemical/mineralogical characteristics would determine the final hydration state of the dehydrated Mg sulfates (section 4.1). A reasonable question would be whether these early established hydration states would change during the long history of Mars. In particular, would the hydration states of Mg sulfates exposed at the surface, and recognition of the original stratigraphy, be affected by obliquity cycles and associated climate changes?

Cycling of obliquity would control the cycles of H₂O ice deposition and sublimation at various regions on Mars, which would in turn stimulate the rehydration and subsequent dehydration of Mg sulfates, which have the highest phase transition rates among Mg, Fe, Ca, and Al sulfates [Wang and Zhou, 2014]. Richardson and Wilson [2002] indicated that when obliquity exceeded 45°, ice sublimation at the polar regions is very high and H₂O ice would occur and persist at the equator of Mars. Calculations by Laskar *et al.* [2004] suggest that the most recent few periods with obliquity >45° occurred between 5.8 and 5.4 Myr ago, with durations of 0.019, 0.028, 0.026, and 0.008 Myr. During those periods, based on our experimental studies on the kinetic properties of Mg sulfates [Wang *et al.*, 2011, 2013], Mg sulfates coexisting with H₂O ice at the Martian surface (or in the shallow subsurface that are in communication with the atmosphere) would equilibrate with H₂O ice (100% RH) and would rehydrate to the highest hydration degree, i.e., meridianiite, MgSO₄·11H₂O (at $T < 2^{\circ}\text{C}$ [Peterson and Wang, 2006]).

We suspect that the time at which the observed hydration states of Mg sulfates at a specific Martian surface location would have been set sometime following the end of the most recent period of high obliquity when the location was covered by H₂O ice. The dehydration of surface Mg sulfates would begin after ice removal by sublimation and would follow the two pathways illustrated in Figure 10, i.e., relatively “clean” Mg sulfate dehydrates to starkeyite and relatively “dirty” Mg sulfate dehydrates to LH-1w. As a result, the stratigraphic order of coexisting LH-1w and starkeyite layers after each obliquity cycle would be controlled by the chemical and mineralogical characteristics of a layer related to the primary precipitation or deposition; i.e., the layering in terms of the prominent Mg sulfate would remain basically unchanged from the early stratigraphic order; except in the case where a major change in catalytic species (e.g., the removal of Fe sulfates by some later atmosphere-surface processes) occurred for a “dirty” layer prior to the latest obliquity cycle.

5. Conclusions

The results from two new experiments suggest additional constraints on the nature and origin of MgSO₄·H₂O (monohydrate) and polyhydrated sulfate observed on Mars. On the basis of these results, we conclude that starkeyite (MgSO₄·4H₂O) is the best candidate for polyhydrated sulfate and that dehydration of highly hydrated Mg sulfates is the origin of the majority of Martian MgSO₄·H₂O (monohydrate) that would take the form of LH-1w, which is different from kieserite.

We conclude that two critical properties of Mg sulfates are responsible for their frequently observed coexistence on Mars. These properties are the following: (1) the metastability of a substructural unit (four-member ring) in starkeyite at relatively low temperatures ($T \leq 50^{\circ}\text{C}$ over Martian history); and (2) catalytic effects associated with coprecipitated species (sulfates, chlorides, oxides, and hydroxides) from chemically complex brines, which can overcome the metastability of starkeyite.

We suggest that a natural combination of the two precipitation processes (Figure 10) is responsible for the broad coexistence of LH-1w and starkeyite layers on Mars. The formation of interbedded sulfate stratigraphy would require multiple inputs of chemically complex brines. The formation of other types of stratigraphic sequences would involve unrelated episodic brine input, whose stratigraphic relationships would depend on brine chemistry, quantity, and input sequence, which are complex functions of climate at the time of deposition, local geochemical characteristics, water-rock ratios, and local geomorphologic features.

In addition to formation related to evaporation of surface waters, MgSO₄·H₂O can form through impact-related or hydrothermal events. When subsurface sulfates (with high hydration degrees [Wang *et al.*, 2013]) are exposed suddenly by impact to a hyperarid Martian atmosphere, rapid subsequent dehydration can bypass the metastability of starkeyite (through amorphization) and form LH-1w directly. Furthermore,

the direct precipitation of kieserite from brine could occur during hydrothermal or volcanic events on Mars, when $\text{Mg-SO}_4\text{-H}_2\text{O}$ brines were available and the temperature exceeded 69°C.

Overall, the structural H_2O held by these two sulfates would represent a large H_2O reservoir at the surface and shallow subsurface on Mars.

Acknowledgments

The data to support the figures and tables in this manuscript and its supporting documents are available at a public website at http://epsc.wustl.edu/~alianwang_papers_data/ and in a sub-folder named as 2016_JGR_wang_paper. This study was supported by a NASA MFRP project NNX10AM89G, NASA support for ExoMars 1295053, ASTEP project NNX09AE80A and contract 08-SC-1072, and MatISSE project NNX13AM22G. The expedition to the Dalangtan (DLT) saline playa on the Tibet Plateau and laboratory analysis of the collected samples were made possible by financial support from the McDonnell Center for Space Science at Washington University in St. Louis. The authors are grateful for many insightful discussions and advice given by R. E. Arvidson and S. McLennan. The overall understanding of the thermodynamics and kinetics properties of major hydrous sulfates was built upon many careful experimental studies in the past 10 years made by the members of the Planetary Spectroscopic group at WUSTL-EPSC, J. J. Freeman, K. Kuebler, Z. X. Peng, Z. C. Ling, W. G. Kong, P. S. Sobron, Y. L. Lu, Y. H. Zhou, J. Wei, and Y. C. Yan. There are no competing financial interests existing for all authors of this manuscript. We appreciate the comments and suggestions given by three anonymous reviewers, which helped greatly the improvement of this manuscript.

References

- Ackiss, S., and J. J. Wray (2014), Occurrences of possible hydrated sulfates in the southern high latitudes of Mars, *Icarus*, **243**, 311–324.
- Arvidson, R. E., F. Poulet, J.-P. Bibring, M. Wolff, A. Gendrin, R. V. Morris, J. J. Freeman, Y. Langevin, N. Mangold, and G. Bellucci (2005), Spectral reflectance and morphologic correlations in eastern Terra Meridiani, Mars, *Science*, **307**, 1591–1594, doi:10.1126/science.1109509.
- Arvidson, R. E., et al. (2010), Spirit Mars Rover mission: Overview and selected results from the northern Home Plate winter haven to the side of Scamander crater, *J. Geophys. Res.*, **115**, E00F03, doi:10.1029/2010JE003633.
- Baur, W. H. (1962), Zur kristallchemie der salzhydrate. Die kristallstrukturen von $\text{MgSO}_4\cdot 4\text{H}_2\text{O}$ (leonhardtite) und $\text{FeSO}_4\cdot 4\text{H}_2\text{O}$ (rozenite), *Acta Crystallogr.*, **15**, 815–826.
- Baur, W. H. (1964), On the crystal chemistry of salt hydrates. II. A neutron diffraction study of $\text{MgSO}_4\cdot 4\text{H}_2\text{O}$, *Acta Crystallogr.*, **17**, 863–869.
- Bibring, J. P., et al. (2004), OMEGA: Observatoire pour la Minéralogie, l'Eau, les Glaces et l'Activité, in *Mars Express: The Scientific Payload*, edited by Andrew Wilson, Scientific Coordination: Agustin Chicarro, ESA SP-1240, pp. 37–49, ESA Publ. Div., Noordwijk, Netherlands.
- Bibring, J. P., et al. (2005), Mars surface diversity as revealed by the OMEGA/Mars Express observations, *Science*, **307**, 1576–1581.
- Bibring, J. P., et al. (2006), Global mineralogical and aqueous Mars history derived from OMEGA/Mars Express data, *Science*, **312**, 400–404.
- Bibring, J. P., et al. (2007), Coupled ferric oxides and sulfates on the Martian surface, *Science*, **317**, 1206–1209.
- Bish, D., et al. (2013), X-ray diffraction results from Mars Science Laboratory: Mineralogy of Rocknest at Gale crater, *Science*, **341**, doi:10.1126/science.1238932.
- Bishop, J. L., et al. (2009), Mineralogy of Juventae Chasma: Sulfates in the light-toned mounds, mafic minerals in the bedrock, and hydrated silica and hydroxylated ferric sulfate on the plateau, *J. Geophys. Res.*, **114**, E00D09, doi:10.1029/2009JE003352.
- Blake, D., et al. (2013), Curiosity at Gale crater, Mars: Characterization and analysis of the Rocknest sand shadow, *Science*, **341**, doi:10.1126/science.1239505.
- Bregeault, J., P. Herpin, J. M. Manoli, and G. Pannetier (1970), Affinement de la structure de la Kieserite $\text{Mg}(\text{SO}_4)(\text{H}_2\text{O})$, *Bull. Soc. Chim. Fr.*, **1970**, 4243–4248.
- Carter, J., F. Poulet, J.-P. Bibring, S. Murchie, V. Ansan, and N. Mangold (2010), Mineralogy of layered deposits in Terby crater, N. Hellas Planitia, 41th LPSC, Abstract 1866.
- Catalano, J. G., A. R. Beehr, and R. Arvidson (2012), Thermodynamic and mass balance constraints on phyllosilicate and evaporite formation scenarios on early Mars, Abstract 7010 for 3rd Conference on Early Mars.
- Catling, D. C., et al. (2006), Light-toned layered deposits in Juventae chasma, Mars, *Icarus*, **181**, 26–51.
- Chio, C. H., et al. (2007), The hydrates and deuterates of ferrous sulfate (FeSO_4): A Raman spectroscopic study, *J. Raman Spectrosc.*, **38**, 87–99.
- Chipera, S. J., and D. T. Vaniman (2007), Experimental stability of magnesium sulfate hydrates that may be present on Mars, *Geochim. Cosmochim. Acta*, **71**, 241–250.
- Chou, I. M., and R. R. Seal II (2003), Determination of epsomite–hexahydrite equilibria by the humidity-buffer technique at 0.1 MPa with implications for phase equilibria in the system $\text{MgSO}_4\text{-H}_2\text{O}$, *Astrobiology*, **3**, 619–630.
- Chou, I. M., and R. R. Seal II (2007), Magnesium and calcium sulfate stabilities and the water budget of Mars, *J. Geophys. Res.*, **112**, E11004, doi:10.1029/2007JE002898.
- Clark, B. C., and D. C. Van Hart (1981), The salts of Mars, *Icarus*, **45**, 370–378.
- Clark, B. C., et al. (2005), Chemistry and mineralogy of outcrops at Meridiani Planum, *Earth Planet. Sci. Lett.*, **240**(1), 72–94.
- Dobrea, E. Z. N., F. Poulet, and M. C. Malin (2008), Correlations between hematite and sulfates in the chaotic terrain east of Valles Marineris, *Icarus*, **193**, 516–534.
- Ehlmann, B. L., J. F. Mustard, G. A. Swayze, R. N. Clark, and J. L. Bishop (2009), Identification of hydrated silicate minerals on Mars using MRO-CRISM: Geologic context near Nili Fossae and implications for aqueous alteration, *J. Geophys. Res.*, **114**, E00D08, doi:10.1029/2009JE003339.
- Farrand, W. H., T. D. Glotch, J. W. Rice Jr., J. A. Hurowitz, and G. A. Swayze (2009), Discovery of jarosite within the Mawrth Vallis region of Mars: Implications for the geologic history of the region, *Icarus*, **204**, 478–488.
- Fishbaugh, K., and J. Head III (2005), Origin and characteristics of the Mars north polar basal unit and implications for polar geologic history, *Icarus*, **174**, 444–474, doi:10.1016/j.icarus.2004.06.021.
- Fishbaugh, K. E., F. Poulet, V. Chevrier, Y. Langevin, and J. P. Bibring (2007), On the origin of gypsum in the Mars north polar region, *J. Geophys. Res.*, **112**, E07002, doi:10.1029/2006JE002862.
- Flahaut, J., C. Quantin, P. Allemand, P. Thomas, and L. Le Deit (2010), Identification, distribution and possible origins of sulfates in Capri Chasma (Mars), inferred from CRISM data, *J. Geophys. Res.*, **115**, E11007, doi:10.1029/2009JE003566.
- Gellert, R., et al. (2006), Alpha Particle X-Ray Spectrometer (APXS): Results from Gusev crater and calibration report, *J. Geophys. Res.*, **111**, E02S05, doi:10.1029/2005JE002555.
- Gendrin, A., et al. (2005), Sulfates in Martian layered terrains: The OMEGA/Mars Express view, *Science*, **307**, 1587–1591, doi:10.1126/science.1109087.
- Greenspan, L. (1977), Humidity fixed points of binary saturated aqueous solutions, *J. Res. Natl. Bur. Stand. U. S., Sect. A*, **81**, 89–96.
- Harri, A.-M., et al. (2014), Mars Science Laboratory relative humidity observations: Initial results, *J. Geophys. Res. Planets*, **119**, 2132–2147, doi:10.1002/2013JE004514.
- Haskin, L. A., et al. (2005), Water alteration of rocks and soils on Mars at the Spirit Rover site in Gusev crater, *Nature*, **436**, 66–69, doi:10.1038/nature03640.
- Hawthorne, F. C., L. A. Groat, M. Raudsepp, and T. S. Ercit (1987), Kieserite, $\text{Mg}(\text{SO}_4)(\text{H}_2\text{O})$, a titanite-group mineral, *Neues Jahrb. Mineral. Abh.*, **157**, 121–132.
- Horgan, B. H., J. F. Bell III, E. Z. Noe Dobrea, E. A. Cloutis, D. T. Bailey, M. A. Craig, L. H. Roach, and J. F. Mustard (2009), Distribution of hydrated minerals in the north polar region of Mars, *J. Geophys. Res.*, **114**, E01005, doi:10.1029/2008JE003187.

- Hurowitz, J. A., S. M. McLennan, N. J. Tosca, R. E. Arvidson, J. R. Michalski, D. W. Ming, C. Schröder, and S. W. Squyres (2006), In situ and experimental evidence for acidic weathering of rocks and soils on Mars, *J. Geophys. Res.*, *111*, E02519, doi:10.1029/2005JE002515.
- Kong, W. G., A. Wang, J. J. Freeman, and P. Sobron (2011), A comprehensive spectroscopic study of synthetic Fe²⁺, Fe³⁺, Mg²⁺, Al³⁺ copiapite by Raman, XRD, LIBS, MIR and vis-NIR, *J. Raman Spectrosc.*, *42*, 1120–1129, doi:10.1002/jrs.2790.
- Kounaves, S. P., et al. (2010), Soluble sulfate in the Martian soil at the Phoenix landing site, *Geophys. Res. Lett.*, *37*, L09201, doi:10.1029/2010GL042613.
- Langevin, Y., F. Poulet, J.-P. Bibring, and B. Gondet (2005), Sulfates in the northern polar region of Mars detected by OMEGA/Mars Express, *Science*, *307*, 1584–1586, doi:10.1126/science.1109091.
- Laskar, J., A. C. M. Correia, M. Gastineau, F. Joutel, B. Levrard, and P. Robutel (2004), Long term evolution and chaotic diffusion of isolation quantities of Mars, *Icarus*, *170*, 343–364.
- Lichtenberg, K. A., et al. (2010), Stratigraphy of hydrated sulfates in the sedimentary deposits of Aram Chaos, Mars, *J. Geophys. Res.*, *115*, E00D17, doi:10.1029/2009JE003353.
- Lide, D. R. (2001), *CRC Handbook of Chemistry and Physics*, 82nd ed., CRC Press, London.
- Ling, Z. C., and A. Wang (2010), A Systematic spectroscopic study of eight hydrous ferric sulfates relevant to Mars, *Icarus*, *209*, 422–433, doi:10.1016/j.icarus.2010.05.009.
- Liu, X. Q., K. Q. Cai, and S. S. Yu (2002), Geochemical simulation of formation and evolution of salt lakes and their water sources in Qardam Basin: Application of Pitzer's model, *Geochimica*, *31*, 501–506.
- Liu, Y., and A. Wang (2015), Dehydration of Na-jarosite, ferricopiapite, and rhomboclase at temperatures of 50°C and 95°C: Implications for Martian ferric sulfates, *J. Raman Spectrosc.*, *10*, doi:10.1002/jrs.4655.
- Liu, Y., R. E. Arvidson, M. J. Wolff, M. T. Mellon, J. G. Catalano, A. Wang, and J. L. Bishop (2012), Lambert albedo retrieval and analyses over Aram Chaos from OMEGA hyperspectral imaging data, *J. Geophys. Res.*, *117*, E00J11, doi:10.1029/2012JE004056.
- Mangold, N., et al. (2007), Mineralogy of the Nilii Fossae region with OMEGA/Mars Express data: 2. Aqueous alteration of the crust, *J. Geophys. Res.*, *112*, E08S04, doi:10.1029/2006JE002835.
- Mangold, N., A. Gendrin, B. Gondet, S. LeMouelic, C. Quantin, V. Ansan, J.-P. Bibring, Y. Langevin, P. Masson, and G. Neukum (2008), Spectral and geological study of the sulfate-rich region of West Candor Chasma, Mars, *Icarus*, *194*(2), 519–543.
- Massé, M., et al. (2008), Mineralogical composition, structure, morphology, and geological history of Aram Chaos crater fill on Mars derived from OMEGA Mars Express Data, *J. Geophys. Res.*, *C115*, E12006, doi:10.1029/2008JE003131.
- McCullom, T. M., B. L. Ehlmann, A. Wang, B. M. Hynek, and T. S. Berquó (2014), Detection of iron substitution in natroalunite-natrojarosite solid solutions and potential implications for Mars, *Am. Mineral.*, *99*(5–6), 948–964, doi:10.2138/am.2014.4617.
- McLennan, S. M. (2012a), Constraints on the age, composition and size of the Martian sedimentary MASS, 43rd LPSC, Abstract 1869.
- McLennan, S. M. (2012b), Geochemistry of sedimentary processes on Mars, sedimentary geology of Mars, SEPM Special Publication No. 102, Print ISBN 978-1-56576-312-8, CD/DVD ISBN 978-1-56576-313-5, p. 119–138.
- McLennan, S. M., et al. (2013), Elemental geochemistry of sedimentary rocks at Yellowknife Bay, Gale Crater, Mars, *Science*, *343*, doi:10.1126/science.1244734.
- McSween, Y. H., et al. (1999), Chemical, multispectral, and textural constraints on the composition and origin of rocks at the Mars Pathfinder landing site, *J. Geophys. Res.*, *104*(E4), 8679–8715, doi:10.1029/98JE02551.
- Milliken, R. E., G. A. Swayze, R. E. Arvidson, J. L. Bishop, and R. N. Clark (2008), Opaline silica in young deposits on Mars, *Geology*, *36*, 847–850.
- Murchie, S. L., et al. (2007), Compact Reconnaissance Imaging Spectrometer for Mars (CRISM) on Mars Reconnaissance Orbiter (MRO), *J. Geophys. Res.*, *112*, E05S03, doi:10.1029/2006JE002682.
- Murchie, S. L., et al. (2009), Evidence for the origin of layered deposits in Candor Chasma, Mars, from mineral composition and hydrologic modeling, *J. Geophys. Res.*, *114*, E00D05, doi:10.1029/2009JE003343.
- Nesbitt, H. W., and R. E. Wilson (1992), Recent chemical weathering of basalts, *Am. J. Sci.*, *292*, 740–777.
- Peterson, R. C., and R. Wang (2006), Crystal molds on Mars: Melting of a possible new mineral species to create Martian chaotic terrain, *Geology*, *34*, 957–960.
- Richardson, M. I., and R. J. Wilson (2002), Investigation of the nature and stability of the Martian seasonal water cycle with a general circulation model, *J. Geophys. Res.*, *107*(E5), 5031, doi:10.1029/2001JE001536.
- Roach, L. H., J. F. Mustard, S. L. Murchie, J.-P. Bibring, F. Forget, K. W. Lewis, O. Aharonson, M. Vincendon, and J. L. Bishop (2009), Testing evidence of recent hydration state change in sulfates on Mars, *J. Geophys. Res.*, *114*, E00D02, doi:10.1029/2008JE003245.
- Roach, L. H., et al. (2010), Hydrated mineral stratigraphy of Ius Chasma, Valles Marineris, *Icarus*, *206*, 253–268, doi:10.1016/j.icarus.2009.09.003.
- Smith, M. D., et al. (2004), First atmospheric science results from the Mars Exploration Rovers Mini-TES, *Science*, *306*(5702), 1750–1753, doi:10.1126/science.1104257.
- Smith, M. D., M. J. Wolff, N. Spanovich, A. Ghosh, D. Banfield, P. R. Christensen, G. A. Landis, and S. W. Squyres (2006), One Martian year of atmospheric observations using MER Mini-TES, *J. Geophys. Res.*, *111*, E12S13, doi:10.1029/2006JE002770.
- Spanovich, N., M. D. Smith, P. H. Smith, M. J. Wolff, P. R. Christensen, and S. W. Squyres (2006), Surface and near-surface atmospheric temperatures for the Mars Exploration Rover landing sites, *Icarus*, *180*, 314–320, doi:10.1016/j.icarus.2005.09.014.
- Squyres, S. W., et al. (2004), The Opportunity Rover's Athena science investigation at Meridiani Planum, Mars, *Science*, *306*, 1698–1703, doi:10.1126/science.1106171.
- Swayze, G. A., et al. (2008), Discovery of the acid-sulfate mineral alunite in Terra Sirenum, Mars, using MRO CRISM: Possible evidence for acid-saline lacustrine deposits?, *Eos (Suppl.)*, Trans. American Geophysical Union (Fall), 89(53), Abstract P44A-04.
- Tosca, N., and S. M. McLennan (2008), Fe oxidation processes at Meridiani Planum and implications for secondary Fe mineralogy on Mars, *J. Geophys. Res.*, *113*, E05005, doi:10.1029/2007JE003019.
- van't Hoff, J. H., et al. (1912), *Untersuchungen U"ber die Bildungsverha"ltnisse der Ozeanischen Salzablagerungen Insbesondere des Stassfurter Saltzlagers*, 239 pp., Akad. Verlagsgesellschaft, Leipzig, Germany.
- Vaniman, D. T., and S. J. Chipera (2006), Transformations of Mg- and Ca-sulfate hydrates in Mars regolith, *Am. Mineral.*, *91*, 1628–1642.
- Vaniman, D. T., D. L. Bish, S. J. Chipera, C. I. Fialips, J. W. Carey, and W. C. Feldman (2004), Magnesium sulphate salts and the history of water on Mars, *Nature*, *431*, 663–665.
- Vaniman, D. T., et al. (2013), Mineralogy of a mudstone at Yellowknife Bay, Gale Crater, Mars, *Science*, *24*, doi:10.1126/science.1243480.
- Wang, A., and K. Connor (2014), Stability fields of hydrous ferrous sulfates and their pathways in dehydration-rehydration processes, Abstract 1070 for 8th International Conference on Mars.
- Wang, A., and Y. Zhou (2014), Experimental comparison of the pathways and rates of the dehydration of Al-, Fe-, Mg-, and Ca-sulfates under Mars relevant conditions, *Icarus*, *234*, 162–173.

- Wang, A., et al. (2006a), Sulfate deposition in subsurface regolith in Gusev Crater, Mars, *J. Geophys. Res.*, *111*, E02S17, doi:10.1029/2005JE002513.
- Wang, A., J. F. Freeman, B. L. Jolliff, and I. M. Chou (2006b), Sulfates on Mars: A systematic Raman spectroscopic study of hydration states of magnesium sulfates, *Geochim. Cosmochim. Acta*, *70*, 6118–6135.
- Wang, A., J. J. Freeman, and B. L. Jolliff (2009), Phase transition pathways of the hydrates of magnesium sulfate in the temperature range 50°C to 5°C: Implication for sulfates on Mars, *J. Geophys. Res.*, *114*, E04010, doi:10.1029/2008JE003266.
- Wang, A., J. J. Freeman, I. M. Chou, and B. L. Jolliff (2011), Stability of Mg-sulfates at –10°C and the rates of dehydration/rehydration processes under Mars relevant conditions, *J. Geophys. Res.*, *16*, E12006, doi:10.1029/2011JE003818.
- Wang, A., W. C. Feldman, M. T. Mellon, and M. P. Zheng (2013), The preservation of subsurface sulfates with mid-to-high degree of hydration in equatorial regions on Mars, *Icarus*, *226*, 980–991.
- Wang, A., P. Sobron, M. Zheng, F. Kong, N. Ma, and Y. Zhao (2014), Preservation of highly hydrated salts in subsurface at a hyperarid region on Tibet plateau, Abstract 2636 for 45th Lunar and planetary Science Conference, Houston, Tex.
- Weitz, C. W., E. Z. Noe Dobrea, M. D. Lane, and A. T. Knudson (2012), Geologic relationships between gray hematite, sulfates, and clays in Capri Chasma, *J. Geophys. Res.*, *117*, E00J09, doi:10.1029/2012JE004092.
- Wendt, L., C. Gross, T. Kneissl, M. Sowe, J.-P. Combe, L. LeDeit, P. C. McGuire, and G. Neukum (2011), Sulfates and iron oxides in Ophir Chasma, Mars, based on OMEGA and CRISM observations, *Icarus*, *213*, 86–103, doi:10.1016/j.icarus.2011.02.013.
- Wiseman, S. M., R. E. Arvidson, R. V. Morris, F. Poulet, J. C. Andrews-Hanna, J. L. Bishop, S. L. Murchie, F. P. Seelos, D. Des Marais, and J. L. Griffes (2010), Spectral and stratigraphic mapping of hydrated sulfate and phyllosilicate-bearing deposits in northern Sinus Meridiani, Mars, *J. Geophys. Res.*, *115*, E00D18, doi:10.1029/2009JE003354.
- Wray, J. J., S. L. Murchie, S. W. Squyres, F. P. Seelos, and L. L. Tornabene (2009), Diverse aqueous environments on ancient Mars revealed in the southern highlands, *Geology*, *37*, 1043–1046, doi:10.1130/G30331A.
- Wray, J. J., S. W. Squyres, L. H. Roach, J. L. Bishop, J. F. Mustard, and E. Z. Noe Dobrea (2010), Identification of the Ca-sulfate bassanite in Mawrth Vallis, Mars, *Icarus*, *209*, 416–421.
- Wray, J. J., et al. (2011), Columbus crater and other possible groundwater-fed paleolakes of Terra Sirenum, Mars, *J. Geophys. Res.*, *116*, E01001, doi:10.1029/2010JE003694.